

SPATIAL DISTRIBUTIONS IN GROUNDWATER DISCHARGE ON VARIOUS TIDAL FLATS IN A SMALL AND STEEP ISLAND, WESTERN JAPAN

Shingo Nozaki¹, *Shin-ichi Onodera¹, Yusuke Tomozawa¹ and Mitsuyo Saito²

¹Graduate School of Advanced Science and Engineering, Hiroshima University, Japan

² Graduate School of Environmental and Life Science, Okayama University, Japan

* Corresponding Author, Received: 16 Jun. 2020, Revised: 13 Jan. 2021, Accepted: 13 Feb. 2021

ABSTRACT: To manage and conserve the seagrass bed and ecosystem in tidal flats, this study examined to confirm spatial distribution in groundwater (SGD) on tidal flats with the area of around 100 m square in a small and steep island. Various groundwater and nutrient discharges were observed at the W and E sites. 1) Based on the water budget, the groundwater flux was estimated to be 8.68 m/yr or 23.9 mm/day in E, and 17.75 m/yr or 48.6 mm/day in W, respectively. 2) Spatial distributions of groundwater contribution ratio (%) in pore water at W was around 60% in average, which was 8 times of that in E site. 3) The NO₃-N concentration in pore water at W site was about 30 times of that at E because of the low attenuation rate with high groundwater velocity. 4) The temporal variation in groundwater flux with tidal fluctuation indicated 2.5 m/day in maximum and -4.0 m/day in minimum. This huge difference between the average flux and maximum indicated also large seawater recirculation and heterogeneous distribution of SGD. This heterogeneous distribution at this tidal flat would contribute to the activity of seagrass and diversity of ecosystem.

Keywords: Submarine groundwater discharge, Spatial distribution, Tidal flat, Island

1. INTRODUCTION

The tidal flats and shallow coastal areas are naturally covered by seaweed and seagrass, these area contributes to biodiversity in the ecosystem [1]. One of the reasons for the rich seagrass bed from the tidal flat to the shallow bottom in a coastal zone is various physical and chemical environments. Submarine groundwater discharge (SGD) defined as any flow of water at land margins from the seabed to the coastal ocean [2,3] has spatial distribution in the km scale and includes fresh groundwater with the stable temperature [4,5]. SGD has significant impacts is an important source of not only freshwater [2,3] but nutrients [6-8].

Recently, the coastal ecosystem such as coral reef and seagrass bed has been degraded by the development and overuse of coastal zone [9]. Because the degradation of seagrass bed causes biodiversity loss in coastal zones, this is one of global environmental issues [10]. In urban regions, the huge nutrient supply from the sewage plant [11], the recycling of accumulated nutrient in sea bed [12] by the tidal pumping [13] caused the eutrophic condition and was degraded ecosystem. In addition, the groundwater depression by over pumping in the coastal city caused seawater intrusion and stop of SGD [14-16].

On the other hand, in the rural regions, the contribution of SGD and coastal current controls

the nutrient and freshwater supply. The groundwater discharge into the sea bed near shore line has conceptually been understood [8,17]. However, spatial variation of SGD in a tidal flat scale has not been clarified enough [18,19].

The purpose of this study was to confirm spatial distribution in groundwater (SGD) and nutrient discharge on tidal flat with the area of around 100m square in a small and steep island.

2. METHOD

2.1 Study Area

The experimental sites were located on Ikuchi Island in Onomichi City, Hiroshima Prefecture, in the central Seto Inland Sea, western Japan. (Fig. 1). The regional climate is warm (average temperature of 15.6°C), with less precipitation in Japan (approx. 1100mm/y). Ikuchi Island is one of the most famous and important orange and citrus production areas. The orange groves cover 42% of the total catchment area, and are mostly located in the downstream area. Forests cover 43% of the upper area. Groundwater resources are important water supply resources for irrigation. However, due to the small annual precipitation with large inter-annual variation, and steep sloping topography, the island faces a risk of water shortage, especially in the drought season.

Ikuchi Island is characterized by a steep terrain and granite bedrock [20], and the total area is 32.7 km². The alluvial fan and plain in the coastal zone is narrow, but is generally deposited by the sediment composed of gravel and sand including clay with the thickness of around 15m [8,20,21].

The research catchments (E and W catchments) are located in the southern area of the island (Fig. 1), and are approximately 1700 m and 900 m in length, and 300 m and 150 m in width, with an area of 0.434 km² and 0.242 km², respectively. These catchments have steep slopes, particularly in the upstream mountainous area, with a top elevation of 396 m and 472 m in E and W catchments, respectively. And experimental tidal flats (E and W) have about 75 m and 30 m in length and 100 m and 250 m in width, respectively. E experimental tidal flat is at the edge of the alluvial fan made by a small stream with 1.5 km in length and it is a half of groundwater discharge area of the catchment. W experimental tidal flat is at the mountain slop foot with the twice average slope gradient of the E catchment and it is similar to the discharge area of the catchment.

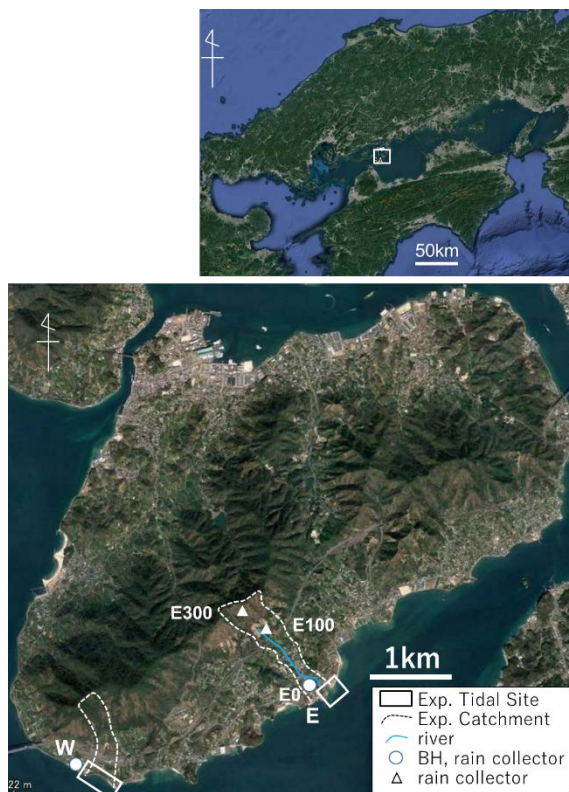


Fig.1 Study area and the experimental sites.

2.2 Field Observation

10 and 17 piezometers on two experimental tidal flats, which is composed of E site (100 m x 30 m) at the alluvial fan edge of an experimental catchment and W sites at the steep mountain slop

foot (300 m x 30 m) were installed with the depth of 50cm, respectively. Pore water samples were collected in December in 2018 and July and December in 2019. Water temperature and electric conductivity (EC) were measured in situ, using the potable meter. In addition, water levels were monitored in 2017 and 2019, rain water and groundwater samples were collected monthly at each catchment.

The water budgets were estimated by the previous researches [21,22] in E catchment based on the river discharge and groundwater monitoring in 2003 and 2004. On the other hand, there is no stream discharge in W catchment.

2.3 Laboratory Analysis

These water samples were filtered using 0.2 µm cellulose ester filters in the field and stored in a freezer until analysis. The stable isotope ratio and nutrient concentration of water samples were analyzed, using the WS-CRDS method (Picarro Company, L2120-i) and a spectrophotometric auto-analyzing system (SWAAT; BL TEC K. K., Japan), respectively.

3. RESULTS AND DISCUSSION

3.1 Water Budget

Table 1 Water Budget in each catchment.

	E catchment	W catchment
P (mm)	1100	1100
Ev (mm)	350 ^[22] - 550 ^[21]	550
Qr (mm)	250 ^[21] - 435 ^[22]	0
Qg (mm)	300 ^[21] - 315 ^[22]	550

Note: [21] using hydrological observation, and [22] using SWAT model.

Water budget is represented as Eq. (1),

$$P - Ev = Qr + Qg + \Delta \quad (1)$$

where P is precipitation, Ev is evapotranspiration, Qr is river discharge, and Qg is groundwater discharge, respectively. The water budgets in E catchment were estimated, using the hydrological observation and monitoring [21] and SWAT model analysis [22]. The water budgets in E and W catchments are shown in Table 1.

Based on the water budget, groundwater discharge in W is twice of E. The catchment area in E is twice of W, and the groundwater discharge volume in E is estimated to be similar to that in W. As the E tidal flat is a half of the discharge area of this catchment, the discharge volume in E site is a half of W tidal flat. If the groundwater discharges

to the experimental tidal flat area (7,500 m²), annual groundwater discharge is estimated to be 8.68 m³/yr or 23.9 mm/day in E, and 17.75 m³/yr or 48.6 mm/day in W, respectively.

3.2 Spatial Distribution of Groundwater Discharge

Figure 2a and 2b shows the distribution of EC in pore water at E and W site, respectively. The average EC at E is 46 mS/cm and that at W is 25 mS/cm. The average groundwater discharge rate at E site was a half of that at W site, the trend of the EC distribution in pore water was similar to the trend of groundwater flux.

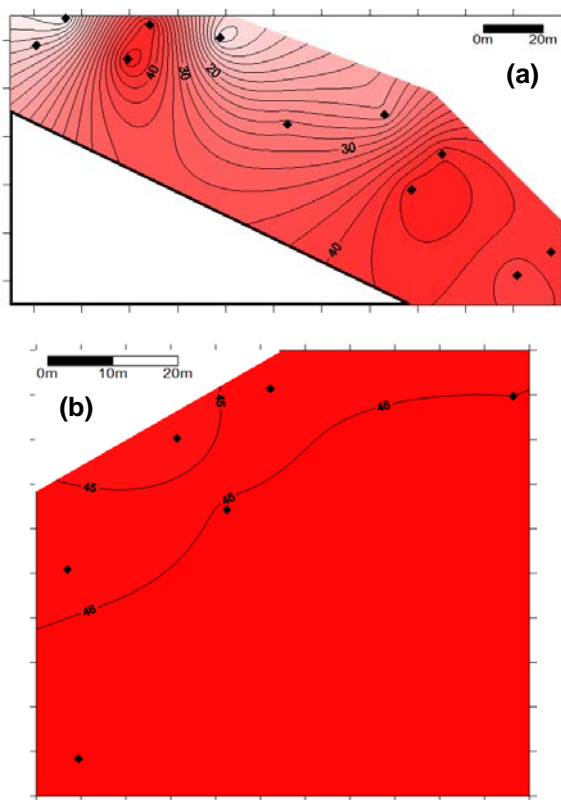


Fig.2 Spatial distributions of EC in pore water at W tidal flat (a) and E (b). The unit is mS/cm. ◆; piezometer plot.

Figure 3 shows the spatial distribution of groundwater contribution ratio (%) in pore water at W and E site. The ratio at W is around 60% in average and the range of from 10% to more than 95%, whereas the ratio at E is around 7% in average and the range from 5% to 10%, respectively. The ratio at W site is 8 times of that in E site. These difference could not explain only by the fresh groundwater flux described above. This means the sea water recirculation flux by the tidal pumping at E site would be around 4 times of that at W site. In general, this flux is related to the

length of the tidal flat, especially the length at E was 2.5 times of that at W.

The distribution at W site is heterogeneous and the pore water with the ratio of 10% were found at 2 piezometers in 17 plots while that with more than 50% and 90% were found at 4 and 1 plots, respectively. On the other hand, the distribution at E site is homogeneous and the ratio continuously decreased from 10% near the land to 5% in the offshore. These comparative trends were shown obviously in the histogram (Fig. 4).

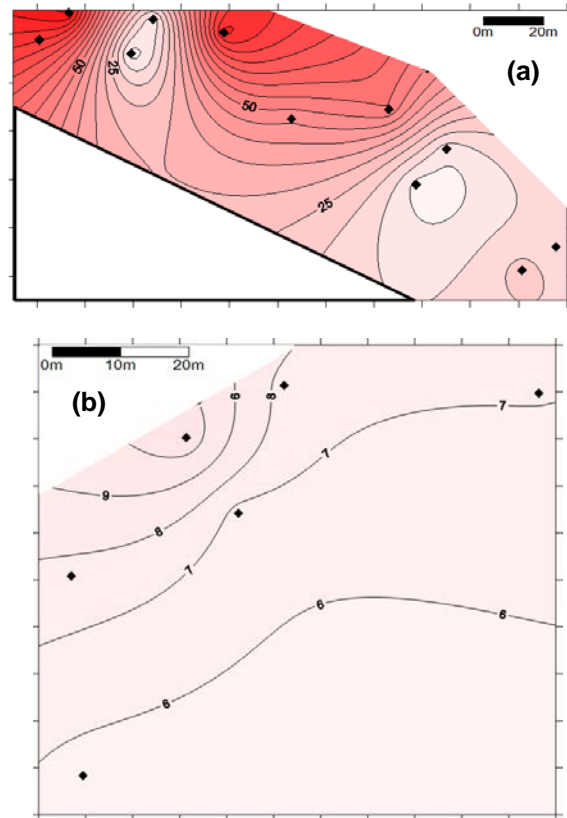


Fig.3 Spatial distribution of groundwater contribution ratio (%) in pore water at W site (a) and E site (b). ◆; piezometer plot.

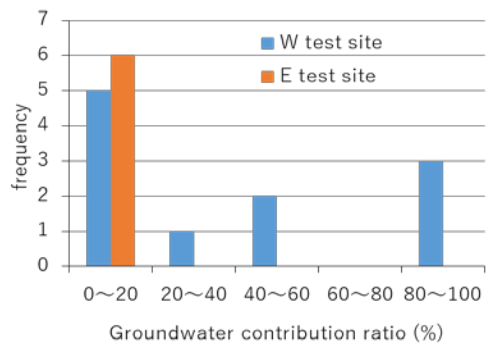


Fig. 4 The histogram of groundwater contribution ratio at E and W site.

3.3 Spatial Distribution of Nutrient Discharge

Spatial distribution of $\text{NO}_3\text{-N}$ concentration (mg/l) in pore water at W site (a) and E site are shown in Fig. 5 (a) and (b), respectively. The lower areas of both catchments are covered by the citrus plantation, and dissolved nitrogen and phosphorus was contained so much in fresh groundwater by leaching of fertilizer component [21]. The concentration distributed the range from 0 mg/l to 7 mg/l at W tidal flat site, whereas it distributed the range from 0 mg/l to 0.2 mg/l. The maximum concentration at W was about 30 times of that at E. This means the attenuation rate is relatively small at W site because of the higher groundwater velocity, as compared at E. Especially, the concentration was maximum at the central part of W site.

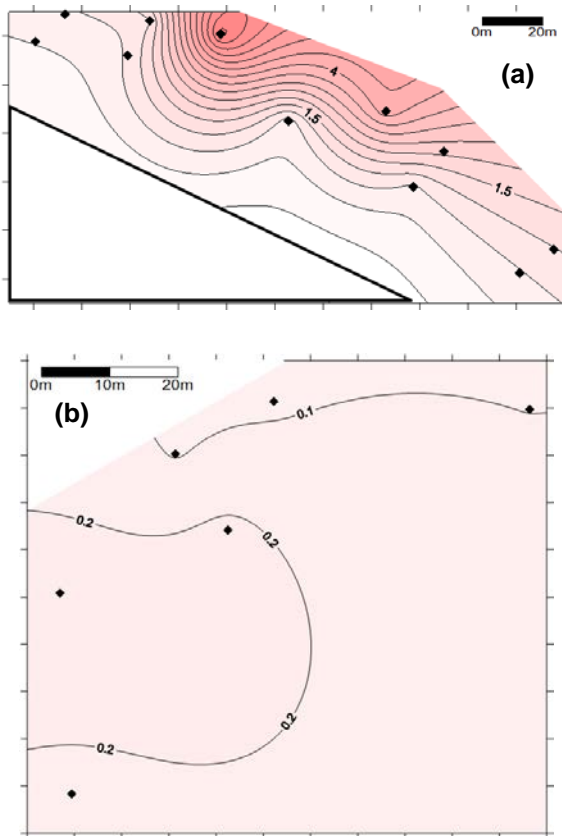


Fig. 5 Spatial distribution of $\text{NO}_3\text{-N}$ concentration (mg/l) in pore water at W site (a) and E site (b). \blacklozenge ; piezometer plot.

Figure 6 shows spatial distributions of SiO_2 concentration (mg/l) in pore water at W site (a) and E site (b). The concentration distributed the range from 3 mg/l to 17 mg/l at W site, whereas it distributed the range from 3 mg/l to 6 mg/l. The plots with high concentration indicated high

contribution of fresh groundwater. The maximum concentration at W was about 3 times of that at E. This means recirculating seawater at E site contained relatively high concentration of SiO_2 because of the supply by the river. In addition, the variation of concentration was obviously smaller than NO_3^- concentration.

3.4 Temporal Variation in Pore Water Pressure and EC

Figure 7 shows the temporal variation in groundwater flux with tidal variation during 3 days. The range of tidal variation was 3.5m. The groundwater flux is maximum at the mid tide during the decreasing tide and minimum at the mid tide during the increasing tide. Figure 8 shows the temporal variation in EC of the pore water with tidal variation. The EC increased with the tidal level, and the tidal pumping effect was indicated [3,4]. But the variation range is only less than 1mS/cm with 34 mS/cm in the average.

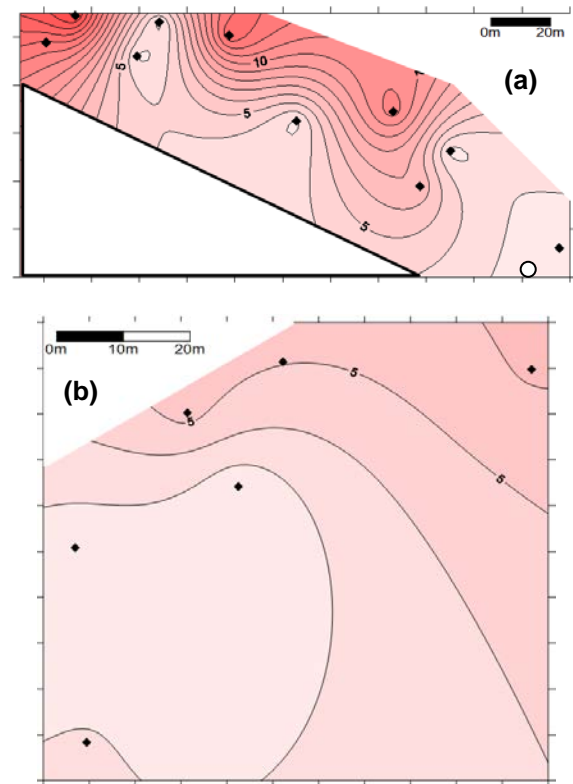


Fig. 6 Spatial distribution of SiO_2 concentration (mg/l) in pore water at W site (a) and E site (b). \blacklozenge ; piezometer plot. \circ ; piezometer plot monitored water level and EC shown in Fig.7 and 8.

The groundwater flux was 2.5 m/day in maximum and -4.0 m/day in minimum. This maximum value was 100 times of the average flux

estimated based on water budget. The negative value during the increasing tide indicated seawater recirculation. The sum for three days showed the positive value, while based on the huge difference between the average flux and maximum indicated also large recirculation and heterogeneous distribution of SGD. This heterogeneous distribution at W site would contribute to the diversity of this ecosystem on the tidal flat. Recently, seagrass biomass is still active at W site as compared with that at E site.

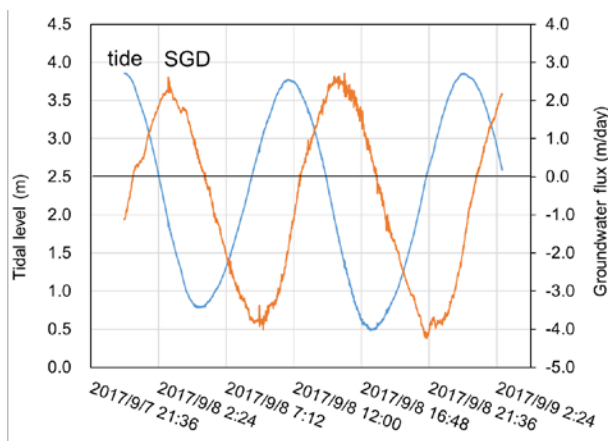


Fig. 7 Temporal variations in tidal level and groundwater flux at the eastern part of Site W (shown in Fig.6).

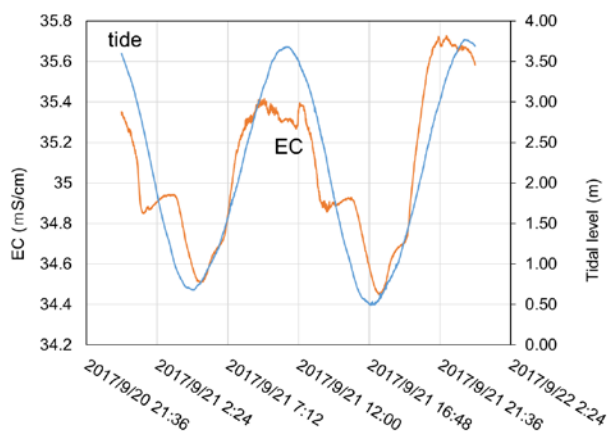


Fig. 8 Temporal variations in tidal level and EC at the eastern part of Site W (shown in Fig.6).

4. CONCLUDING REMARKS

This study examined to confirm spatial distribution in groundwater (SGD) on tidal flats with the area of around 100m square in a small and steep island.

1) Based on the water budget, the groundwater flux was estimated to be 8.68 m/yr or 23.9

mm/day in E, and 17.75 m/yr or 48.6 mm/day in W, respectively.

- 2) Spatial distributions of groundwater contribution ratio (%) in pore water at W was around 60% in average, which was 8 times of that in E site.
- 3) The NO₃-N concentration in pore water at W site was about 30 times of that at E because of the low attenuation rate with high groundwater velocity.
- 4) The temporal variation in groundwater flux with tidal fluctuation indicated 2.5m/day in maximum and -4.0m/day in minimum. This huge difference between the average flux and maximum indicated also large seawater recirculation and heterogeneous distribution of SGD. This heterogeneous distribution at this tidal flat would contribute to the activity of seagrass and diversity of ecosystem.

5. ACKNOWLEDGMENTS

This research was supported by JSPS KAKENHI Grant 18H04151 and 18H03411. We appreciate the reviewers and editors for their suggestions, and Ms. Morita and Mr. Hanioka for their cooperation.

6. REFERENCES

- [1] Duffy J. E., Biodiversity and the functioning of seagrass ecosystems. *Marine Ecology Prog. Ser.*, 311, 2006, pp.233-250.
- [2] Taniguchi M., Burnett W. C., Cable J. E., and Turner J. V., Investigation of submarine groundwater discharge. *Hydrol. Process.*, 16, 2002, pp.2115-2129.
- [3] Burnett W. C., Aggarwal P. K., Aureli A., Bokuniewicz H., Cable J. E., Charette M. A., Kontar E., Krupa S., Kulkarni K. M., Loveless A., 2006. Quantifying submarine groundwater discharge in the coastal zone via multiple methods. *Sci. Total Environ.*, 367, 2-3, 498-543.
- [4] Burnett W. C., Dulaiova, H., Radon as a tracer of submarine groundwater discharge into a boat basin in Donnalucata, Sicily. *Cont. Shelf Res.*, 26, 7, 2006, pp.862-873.
- [5] Saito M., Onodera S., Guo X. Y., Seasonal variation of the ²²²Rn concentration in the Central part of the Seto Inland Sea, Japan. *Interdisc. Stud. Environ. Chem. Terrapub*, 6, 2012, pp.339-344.
- [6] Santos I. R., Burnett W. C., Dittmar T., Suryaputra I. G. N. A., Chanton J., Tidal pumping drives nutrient and dissolved organic matter dynamics in a Gulf of Mexico subterranean estuary. *Geochim. Cosmochim. Acta*, 73, 5, 2009, pp.1325-1339.

- [7] Kim G., Kim J. S., Hwang D. W., Submarine groundwater discharge from oceanic islands standing in oligotrophic oceans: implications for global biological production and organic carbon fluxes. *Limnol. Oceanogr.*, 56, 2, 2011, pp.673-682.
- [8] Onodera S., Saito M., Hayashi M., Sawano M., Nutrient dynamics with interaction of groundwater and seawater in a beach slope of steep island, western Japan. IAHS Publication, 312, 2007, pp.150-158.
- [9] Climate Technology Centre and Network, Management of seagrass beds. <https://www.ctc-n.org/technologies/management-seagrass-beds#:~:text=Degradation%20is%20due%20to%20smothering,Temperature%20increases>.
- [10] Rockström J., Steffen W., Noone K., Persson A., Chapin F. S., Lambin E. F., Lenton T. M., Scheffer M., Folke C., Schellnhuber H. J., Nykvist B., de Wit C. A., Hughes T., van der Leeuw S., Rodhe H., Sörlin S., Snyder P. K., Costanza R., Svedin U., Falkenmark M., Karlberg L., Corell R. W., Fabry B. J., Hansen J., Walker B., Liverman D., Richardson K., Crutzen P., Foley J. A., A safe operating space for humanity, *Nature*, 461, 2009, pp.472-475.
- [11] Saito M., Onodera S., Jin G., Shimizu Y., Taniguchi M., Nitrogen dynamics in a highly urbanized coastal area of western Japan: impact of sewage-derived loads. *Progress in Earth and Planetary Science*, Volume 5, 2018, DOI: 10.1186/s40645-018-0177-6.
- [12] Jin G., Onodera S., Saito M., and Shimizu Y., Sediment phosphorus cycling in a nutrient-rich embayment in relation to sediment phosphorus pool and release. *Limnology*, 2020, <https://doi.org/10.1007/s10201-020-00627-x>.
- [13] Onodera S., Saito M., Yoshikawa M., Onishi K., Shimizu Y., and Ito H., Nutrient transport and surface water-groundwater interactions in the tidal zone of the Yamato River, Japan. IAHS Publication, 361, 2013, pp.204-211.
- [14] Onodera S., Saito M., Sawano M., Hosono T., Taniguchi M., Shimada J., Umezawa Y., Lubis R. F., Buapeng S., and Delinom R., Effects of intensive urbanization on the intrusion of shallow groundwater into deep groundwater: Examples from Bangkok and Jakarta. *Science of the Total Environment*, 407, 2009, pp.3209-3217.
- [15] Tomozawa Y., Onodera S. and Saito M., Estimation of groundwater recharge and salinization in a coastal alluvial plain and Osaka megacity, Japan using $\delta^{18}\text{O}$, δD , and Cl^- . *International Journal of GEOMATE*, Vol.16, Issue 56, 2019, pp.153-158.
- [16] Rusydi A. F., Saito M., Ioka S., Maria R. and Onodera S., Estimation of ammonium sources in Indonesian coastal alluvial groundwater using Cl^- and GIS. *International Journal of GEOMATE*, Vol.17, Issue 62, 2019, pp.53-58.
- [17] Nakada S., Yasumoto, J., Taniguchi, M., and Ishitobi, T., Submarine groundwater discharge and seawater circulation in a subterranean estuary beneath a tidal flat. *Hydrol. Process.*, 25, 17, 2011, pp.2755-2763.
- [18] Shuler C. K., Dulai H., Leta O. T., Fackrell J., Welch E., and El-Kadi A. I., Understanding surface water-groundwater interaction, submarine groundwater discharge, and associated nutrient loading in a small tropical island watershed. *Journal of Hydrology*, 585, 2020, 124342.
- [19] Zhu A., Saito M., Onodera S., Shimizu Y., Jine G., Ohta T., and Chen J., Evaluation of the spatial distribution of submarine groundwater discharge in a small island scale using the ^{222}Rn tracer method and comparative modeling. *Marine Chemistry*, 209, 2019, pp.25-35.
- [20] Takeuchi T., Onodera S., Yamaguchi K. and Kitaoka K., Estimation of sedimentation rate and fresh-saline environment in a coastal alluvial plain, using boring cores of alluvium in the central part area of Seto Inland Sea, Japan. *International Journal of GEOMATE*, Vol.17, Issue 60, 2019, pp.70-75.
- [21] Saito M., Onodera S., Okubo K., Takagi S., Maruyama Y., Jin G., and Shimizu Y., Effects of physical and morphometric factors on nutrient removal properties in agricultural ponds. *Water Science & Technology*, 72, 12, 2015, pp.2187-2193.
- [22] Jin G., Shimizu Y., Onodera S., Saito M., and Matsumori K., Evaluation of drought impact on groundwater recharge rate using SWAT and Hydrus models on an agricultural island in western Japan. *Proc. Int. Assoc. Hydrol. Sci.*, 371, 2015, pp.143-148.